UNIVERSIDAD DE INVESTIGACIÓN DE TECNOLOGÍA EXPERIMENTAL YACHAY

Escuela de Ciencias Físicas y Nanotecnología

TÍTULO: A connection between gravastar geometries and self gravitating spheres supported by anisotropic fluids

Trabajo de integración curricular presentado como requisito para la obtención del título de Física

Autor:

Carrasco Hidalgo Mikaela Salomé

Tutor:

Ph. D. González Vázquez Gema

Co - Tutor:

Ph. D. Contreras Herrada Ernesto José

Urcuquí, Noviembre 2021

Urcuquí, 11 de noviembre de 2021

SECRETARÍA GENERAL
(Vicerrectorado Académico/Cancillería)
ESCUELA DE CIENCIAS FÍSICAS Y NANOTECNOLOGÍA
CARRERA DE FÍSICA
ACTA DE DEFENSA No. UITEY-PHY-2021-00022-AD

A los 11 días del mes de noviembre de 2021, a las 16:00 horas, de manera virtual mediante videoconferencia, y ante el Tribunal Calificador, integrado por los docentes:

Presidente Tribunal de Defensa	Dr. RAMIREZ VELASQUEZ JOSE MANUEL , Ph.D.
Miembro No Tutor	Dra. ROJAS CELY CLARA INES , Ph.D.
Tutor	Dra. GONZALEZ VAZQUEZ, GEMA , Ph.D.

El(la) señor(ita) estudiante **CARRASCO HIDALGO, MIKAELA SALOME**, con cédula de identidad No. **0401867148**, de la **ESCUELA DE CIENCIAS FÍSICAS Y NANOTECNOLOGÍA**, de la Carrera de **FÍSICA**, aprobada por el Consejo de Educación Superior (CES), mediante Resolución **RPC-SO-39-No.456-2014**, realiza a través de videoconferencia, la sustentación de su trabajo de titulación denominado: **A connection between gravastar geometries and self gravitating spheres supported by anisotropic fluids** , previa a la obtención del título de **FÍSICO/A**.

El citado trabajo de titulación, fue debidamente aprobado por el(los) docente(s):

Tutor	Dra. GONZALEZ VAZQUEZ, GEMA , Ph.D.

Y recibió las observaciones de los otros miembros del Tribunal Calificador, las mismas que han sido incorporadas por el(la) estudiante.

Previamente cumplidos los requisitos legales y reglamentarios, el trabajo de titulación fue sustentado por el(la) estudiante y examinado por los miembros del Tribunal Calificador. Escuchada la sustentación del trabajo de titulación a través de videoconferencia, que integró la exposición de el(la) estudiante sobre el contenido de la misma y las preguntas formuladas por los miembros del Tribunal, se califica la sustentación del trabajo de titulación con las siguientes calificaciones:

Tipo	Docente	Calificación
Tutor	Dra. GONZALEZ VAZQUEZ, GEMA , Ph.D.	10,0
Presidente Tribunal De Defensa	Dr. RAMIREZ VELASQUEZ JOSE MANUEL , Ph.D.	10,0
Miembro Tribunal De Defensa	Dra. ROJAS CELY CLARA INES , Ph.D.	10,0

Lo que da un promedio de: **10 (Diez punto Cero)**, sobre 10 (diez), equivalente a: **APROBADO**

Para constancia de lo actuado, firman los miembros del Tribunal Calificador, el/la estudiante y el/la secretario ad-hoc.

Certifico que *en cumplimiento del Decreto Ejecutivo 1017 de 16 de marzo de 2020, la defensa de trabajo de titulación (o examen de grado modalidad teórico práctica) se realizó vía virtual, por lo que las firmas de los miembros del Tribunal de Defensa de Grado, constan en forma digital.*

CARRASCO HIDALGO, MIKAELA SALOME
Estudiante

JOSE MANUEL RAMIREZ VELASQUEZ
Digitally signed by JOSE MANUEL RAMIREZ VELASQUEZ
Date: 2021.11.16 13:11:29 -05'00'

Dr. RAMIREZ VELASQUEZ JOSE MANUEL , Ph.D.
Presidente Tribunal de Defensa

GEMA GONZALEZ VAZQUEZ
Firmado digitalmente por GEMA GONZALEZ VAZQUEZ
Fecha: 2021.11.16 11:08:28 -05'00'

Dra. GONZALEZ VAZQUEZ, GEMA , Ph.D.
Tutor

Dra. ROJAS CELY CLARA INES , Ph.D.
Miembro No Tutor

CLARA INES ROJAS CELY
Firmado digitalmente por CLARA INES ROJAS CELY
Fecha: 2021.11.16 09:55:17 -05'00'

CIFUENTES TAFUR, EVELYN CAROLINA
Secretario Ad-hoc

EVELYN CAROLINA CIFUENTES TAFUR
Firmado digitalmente por EVELYN CAROLINA CIFUENTES TAFUR
Fecha: 2021.11.16 09:12:48 -05'00'

AUTORÍA

Yo, **MIKAELA SALOMÉ CARRASCO HIDALGO**, con cédula de identidad 0401867148, declaro que las ideas, juicios, valoraciones, interpretaciones, consultas bibliográficas, definiciones y conceptualizaciones expuestas en el presente trabajo; así cómo, los procedimientos y herramientas utilizadas en la investigación, son de absoluta responsabilidad de el/la autora (a) del trabajo de integración curricular. Así mismo, me acojo a los reglamentos internos de la Universidad de Investigación de Tecnología Experimental Yachay.

Urcuquí, noviembre 2021.

Mikaela Salomé Carrasco Hidalgo
CI: 0401867148

AUTORIZACIÓN DE PUBLICACIÓN

Yo, **MIKAELA SALOMÉ CARRASCO HIDALGO** con cédula de identidad 0401867148, cedo a la Universidad de Tecnología Experimental Yachay, los derechos de publicación de la presente obra, sin que deba haber un reconocimiento económico por este concepto. Declaro además que el texto del presente trabajo de titulación no podrá ser cedido a ninguna empresa editorial para su publicación u otros fines, sin contar previamente con la autorización escrita de la Universidad.

Asimismo, autorizo a la Universidad que realice la digitalización y publicación de este trabajo de integración curricular en el repositorio virtual, de conformidad a lo dispuesto en el Art. 144 de la Ley Orgánica de Educación Superior

Urcuquí, noviembre 2021.

Mikaela Salomé Carrasco Hidalgo
CI: 0401867148

Acknowledgements

I express my sincere gratitute to Ernersto Contreras Ph.D who trust in me and help me with a lot of guidance and useful critiques in this graduation project.

I am grateful to all my professors at Yachay Tech University, who were the heroes who shared their knowledge and inspired me to continue learning and who motivated me day by day to be a scientist.

Also, I have to say *thank you* to my mother who encouraged me with her love even in the most difficult times. Finally, I would like to thank my closest friends for supporting me and made my days happier.

Resumen

En el marco de la Relatividad General, el desacople gravitacional ha llegado a ser una herramienta útil para extender las soluciones isótropas a dominios anisótropos. En este trabajo nosotros obtenemos dos nuevas soluciones para objetos ultracompactos a través del desacople gravitacional. Por un lado, nosotros hemos considerado complejidad polinómica y obtuvimos dos modelos diferentes para el interior estelar. Por otra parte, las soluciones fueron bien pegadas con dos vacíos modificados diferentes. La densidad de energía es monótonamente decreciente y el horizonte de eventos de la estrella es ausente, como es requerido.

Palabras Clave: mínima deformación geométrica , vacío deformado, gravastars, complejidad polinomial.

Abstract

In the framework of General Relativity, the gravitational decoupling has become a useful tool to extend isotropic solutions to anisotropic domains. In this work we obtain two new solutions describing ultracompact objects by the gravitational decoupling. On one hand, we have considered a polynomial complexity and obtained two different models for stellar interiors. On the other hand, the solutions have been matched to two different modified vacuums. The energy density is monotonously decreasing and the event horizon of the star is absent as required.

Keywords: minimal geometric deformation, deformed vacuum, gravastars, polynomial complexity.

Contents

List of Figures

Chapter 1

Introduction

The study of Black Holes (BH) in General Relativity (GR) has been one of the most important topics in the scientific literature. Although, Albert Einstein in 1916[1] proposed the principles of GR, it was not until 1960's that the term *Black Hole* was used. Though the BH's are already accepted as astrophysical objects, they continue to be objects of discussion due to the singularity present at its center. However, since they appear to be real, they are often used to test strong gravitational fields, to study gravitational waves[2 3 4] and in the present, owning to the first image taken of a BH, to study its shadows[5 6].

From the mathematical point of view, GR seems to be incomplete due to the singularities that appear in the description of BH's. In this sense, some studies are dedicated to propose new theories, new astrophysical objects similar to BH like regular BH's[7 8 9], traversable wormholes[10 11] and ultracompact stars, or generalizations of the theory[12].

Ultracompact stars or *"gravastars"* were modeled firstly by Mazur and Mottola[13] (MM) by the use of the Schwarzschild interior solution in a special case that was the base for further studies in the recent years[14 15]. Recently, the MM model has been extended to anisotropic domains by the Gravitational Decoupling (GD) through the Minimal Geometric Deformation (MGD) approach[15] and in contrast to the original solution, the resulting configuration can be matched smoothly with a modified vacuum so the thin shell approach can be avoided. In this work we follow the ideas in[15] and construct an anisotropic ultracompact star by using the recently introduced concept of complexity[16].

1.1 Problem Statement

This work is devoted to the study of new solutions for ultracompact stars which mimic the exterior geometry of a BH without singularities nor event horizon. We assume static and spherically symmetric spacetimes so the Einstein field equations correspond to five equations with three unknowns. In order to reduce the number of degrees of freedom we employ the GD by MGD to extent the well known MM gravastar model to anisotropic domains. To close the system of differential equation we implement the concept of complexity of self gravitating spheres.

1.2 General and Specific Objectives

The main goal of this project is twofold. The first one is based on the obtaining of an alternative model for gravastar by the use of a complexity factor for the interior region. The second one is to provide an MGD deformed vacuum for the exterior geometry of the particular configuration taking into account that the exterior region must match with the proposed interior configuration.

This work is organized as follows. In chapter 2 we develop the theoretical background of GR and the basics for the description of gravastars. Chapter 3 is focused on the proposal of two new solutions based on the complexity factor as a polynomial expression for the interior region which will be matched with two exterior geometries by the use of MGD approach. Finally, the conclusions are shown in chapter 4.

In this work, instead of using the CGS units where $G = 6.674\times10^{-8}$ cm$^3/g\ s^2$, c=3 $\times10^{10}$ cm/s, we will be using the Geometrized Unit System where $G = c = 1$ and $\kappa = 8\pi$. Also the signature of the metric will be $(+, -, -, -)$.

Chapter 2

Theoretical Background

In this chapter we summarize the basic elements of GR starting from the Einstein field equations to continue describing both the interior and exterior Schwarzschild solution. Next, we explain the necessary conditions to match the interior with the exterior solutions and then, we review in detail the GD by MGD. Finally, we study complexity in the context of GR and the basics to describe a gravastar.

2.1 General Relativity

GR is a geometric theory of gravitation where gravity is not considered as a force but as a consequence of the curvature of the spacetime itself[17]. The new concept of gravity helps us to describe some problems which could not be explained through classical theories as the bending of light, the precession of the perihelion of Mercury, the gravitational redshift, and the motion of particles around massive objects[18].

GR is based on the equivalence and covariance principles. The first one states tha5 as the inertial and gravitational mass are indistinguishable it is impossible to differentiate between free falling observers and accelerated observes in a small region of spacetime. The second principle remarks the invariance of physical laws under coordinate transformations. The concepts of GR establish that the spacetime where we live is a four dimentioinal pseudo Riemannian . It remarks the difference between a simple Euclidean space $\mathbb{R}^n$ from a pseudo Riemannian space of $(3+1)$ dimensions.

All the information of our spacetime is codified in the Einstein field equations (EFE), which corresponds to a set of ten non linear differential equations for the metric $g_{\mu\nu}$ and represent a connection between the mass and the energy which tell us how the spacetime warp in the presence of matter[1].

2.1.1 Einstein field equations

EFE are given by

$$G_{\mu\nu} = \kappa T_{\mu\nu}, \tag{2.1}$$

where $G_{\mu\nu}$ is the Einstein tensor which encodes information of the geometry of the spacetime, $T_{\mu\nu}$ is the energy momentum tensor which acts as the source of a gravitational field and κ is 8π.

The Einstein tensor can be written as,

$$G_{\mu\nu} = R_{\mu\nu} - \frac{1}{2} R g_{\mu\nu}, \tag{2.2}$$

where $g_{\mu\nu}$ is the metric, which is a symmetric $(0,2)$ rank tensor, $R_{\mu\nu}$ is the Ricci tensor and R is the Ricci scalar that can be written as

$$R = g^{\mu\nu} R_{\mu\nu}, \tag{2.3}$$

$$R_{\mu\nu} = R^{\alpha}_{\mu\alpha\nu}, \tag{2.4}$$

where $R^{\alpha}_{\mu\alpha\nu}$ is the Riemann tensor that, in terms of the Christoffel symbols, reads

$$R^{\lambda}_{\mu\rho\nu} = \partial_{\rho}\Gamma^{\lambda}_{\mu\nu} - \partial_{\nu}\Gamma^{\lambda}_{\mu\rho} + \Gamma^{\lambda}_{\sigma\rho}\Gamma^{\sigma}_{\mu\nu} - \Gamma^{\lambda}_{\sigma\nu}\Gamma^{\sigma}_{\mu\rho}. \tag{2.5}$$

Additionally, the Christoffel symbols can be written as

$$\Gamma^{\nu}_{\lambda\mu} = \frac{1}{2} g^{\nu\sigma}(\partial_{\mu} g_{\sigma\lambda} + \partial_{\lambda} g_{\sigma\mu} - \partial_{\sigma} g_{\mu\lambda}). \tag{2.6}$$

From the definition above the Riemann tensor is endowed with the following symmetries

$$R_{\mu\nu\lambda\rho} = R_{\lambda\rho\mu\nu}, \tag{2.7}$$
$$R_{\mu\nu\lambda\rho} = -R_{\nu\mu\lambda\rho}, \tag{2.8}$$
$$R_{\mu\nu\lambda\rho} = -R_{\mu\nu\rho\lambda}, \tag{2.9}$$
$$R_{\mu\nu\lambda\rho} + R_{\mu\rho\nu\lambda} = -R_{\mu\lambda\rho\nu}. \tag{2.10}$$

In this regard, $G_{\mu\nu}$ is a symmetric tensor and as a consequence, the Einstein equations corresponds to a set of ten second order and coupled differential equations.

The energy momentum tensor encodes the information of the matter content. For an isotropic fluid the energy momentum tensor in the tensorial form reads as [19 20 21]

$$T_{\mu\nu} = (\rho + p)\, U_\mu U_\nu + p g_{\mu\nu}, \tag{2.11}$$

or in a matrix form as,

$$T^\mu_\nu = \begin{pmatrix} \rho & 0 & 0 & 0 \\ 0 & -p & 0 & 0 \\ 0 & 0 & -p & 0 \\ 0 & 0 & 0 & -p \end{pmatrix} \tag{2.12}$$

It is worth mentioning that the energy momentum tensor is covariantly conserved, namely $\nabla_\mu T^{\mu\nu} = 0$.

2.2 Schwarzschild exterior solution

The first exact solution of the Einstein field equations were found by K. Schwarzschild[22] and describe the exterior geometry around a central object in a static and spherically symmetric spacetime. In this section we derive the Schwarzschild exterior solution in some detail. Let us start by assuming a line element parametrized as

$$ds^2 = e^{2\alpha(r)}dt^2 - e^{2\beta(r)}dr^2 - r^2\left[d\theta^2 + \sin^2(\theta)d\phi^2\right], \tag{2.13}$$

where $\left(d\theta^2 + \sin^2(\theta)d\phi^2\right)$ can be also seen as $d\Omega^2$ that acts as the angular part, and $\alpha(r)$ and $\beta(r)$ are functions of the radial coordinate only. Note that the metric (2.13) does not depend explicitly on time and is invariant under rotation as required.

The non vanishing Christoffel symbols associated with the metric (2.13) read

$$\begin{aligned}
\Gamma^t_{tr} =& \partial_r\alpha, \\
\Gamma^\theta_{r\theta} =& 1/r, \\
\Gamma^r_{\phi\phi} =& -re^{-2\beta}\sin^2\theta, \\
\Gamma^r_{tt} =& e^{2(\alpha-\beta)}\partial_r\alpha, \\
\Gamma^r_{\theta\theta} =& -re^{-2\beta}, \\
\Gamma^\theta_{\phi\phi} =& -\sin\theta\cos\theta, \\
\Gamma^r_{rr} =& \partial_r\beta, \\
\Gamma^\phi_{r\phi} =& 1/r, \\
\Gamma^\phi_{\theta\phi} =& \frac{\cos\theta}{\sin\theta},
\end{aligned} \tag{2.14}$$

from where, the components of the Riemann tensor are given by

$$\begin{aligned}
R^{t}_{rtr} =&\partial_r\alpha\partial_r\beta - \partial_r^2\alpha - (\partial_r\alpha)^2,\\
R^{t}_{\theta t\theta} =&- re^{-2\beta}\partial_r\alpha,\\
R^{t}_{\phi t\phi} =&- re^{-2\beta}\sin^2\theta\partial_r\alpha,\\
R^{r}_{\theta r\theta} =&re^{-2\beta}\partial_r\beta,\\
R^{r}_{\phi r\phi} =&re^{-2\beta}\sin^2\theta\partial_r\beta,\\
R^{\theta}_{\phi\theta\phi} =&(1-e^{-2\beta})\sin^2\theta.
\end{aligned} \tag{2.15}$$

Using Eqs. (2.15), the components of the Ricci tensor are

$$\begin{aligned}
R_{tt} =&e^{2(\alpha-\beta)}\left[\partial_r^2\alpha + (\partial_r\alpha)^2 - \partial_r\alpha\partial_r\beta + \frac{2}{r}\partial_r\alpha\right],\\
R_{rr} =&- \partial_r^2\alpha - (\partial_r\alpha)^2 + \partial_r\alpha\partial_r\beta + \frac{2}{r}\partial_r\beta,\\
R_{\theta\theta} =&e^{-2\beta}\left[r(\partial_r\beta - \partial_r\alpha) - 1\right] + 1,\\
R_{\phi\phi} =&\sin^2\theta R_{\theta\theta}.
\end{aligned} \tag{2.16}$$

As we are dealing with a vacuum solution, the components of the Ricci tensor must vanish independently. Then, we can write

$$e^{2(\alpha-\beta)}R_{tt} + R_{rr} = \frac{2}{r}(\partial_r\alpha + \partial_r\beta) = 0, \tag{2.17}$$

from where $\alpha = -\beta + constant$. Now, by a rescaling of the time in the form of $e^{-c}t$, is possible to set the constant to zero. So,

$$\alpha(r) = -\beta(r). \tag{2.18}$$

Setting $R_{\theta\theta} = 0$, it yields

$$e^{2\alpha}(2r\partial_r\alpha + 1) = 1, \tag{2.19}$$

from where

$$e^{2\alpha} = 1 - \frac{R_S}{r}, \tag{2.20}$$

where $R_S = 2M$ is the *Schwarzschild radius**.Finally, the Schwarzschild metric reads

$$ds^2 = \left(1 - \frac{2M}{r}\right)dt^2 - \left(1 - \frac{2M}{r}\right)^{-1}dr^2 - r^2d\Omega. \tag{2.21}$$

*Actually R_S is $2GM/c^2$ and it is found in the weak field case [22]

At this point some comments are in order. First, note that the solution is asymptotically flat, namely, the Minkowski metric is recovered in the limits $r \to \infty$. Second, the parameter M is the mass of the central object which can be identified in the weak field limit approximation. Finally, it is worth noticing that Eq. (2.21) diverges both at $r = R_S$ and $r = 0$. In this regard, the radius of the central object should be $R > R_S$ in order to avoid the singularities of $g_{\mu\nu}$. However, as we shall discuss below, in the study of black holes a detailed discussion about those singularities is compulsory.

2.2.1 Spherically symmetric black hole

In this section we go a step further in the discussion of the metric (2.21) in order to establish the nature of the singularities appearing at $r = R_S$ and $r = 0$.

To this end, we start analyzing the null geodesics ($ds^2 = 0$) where θ and ϕ are constants. Then, we have,

$$\left(1 - \frac{2M}{r}\right) dt^2 - \left(1 - \frac{2M}{r}\right)^{-1} dr^2 = 0, \tag{2.22}$$

$$\frac{dt}{dr} = \pm \left(1 - \frac{2M}{r}\right)^{-1}, \tag{2.23}$$

from where,

$$t_\pm = \pm \left[r + 2M \ln (r - 2M) \right]. \tag{2.24}$$

Note that the plus and minus, represent the slopes of the light cones as can be seen in the figure 2.1†. If a particle goes from $r > 2M$ to $r < 2M$, it will take an infinite time to pass the point $r = 2M$ since the light cone at $r > 2M$ starts closing up and its future world line will go undoubtedly to infinity. Therefore, the particle will never pass the limit at the Schwarzschild radius because it will take an infinite time. Conversely, in the region $r < 2M$ both the timelike and spacelike roles are interchange and as a consequence the worldline of a particle will end unavoidably at the singular point $r = 0$.

An alternative route to evaluate the geometry of singular points is through the invariants constructed as contraction of the Riemann tensor. In the literature, the basic scalars are

$$R = g^{\mu\nu} R_{\mu\nu}, \tag{2.25}$$

$$R^2 = R_{\mu\nu} R^{\mu\nu}, \tag{2.26}$$

$$\mathcal{K} = R_{\mu\nu\lambda\rho} R^{\mu\nu\lambda\rho}, \tag{2.27}$$

which correspond to the Ricci, Ricci squared and the Kretschmann scalar, respectively. Given that the scalars capture all the information encoded in the Riemann tensor, we say that a point is a real singularity whenever some of the

†Actually, the light cone can be described by the intersection of the null geodesics

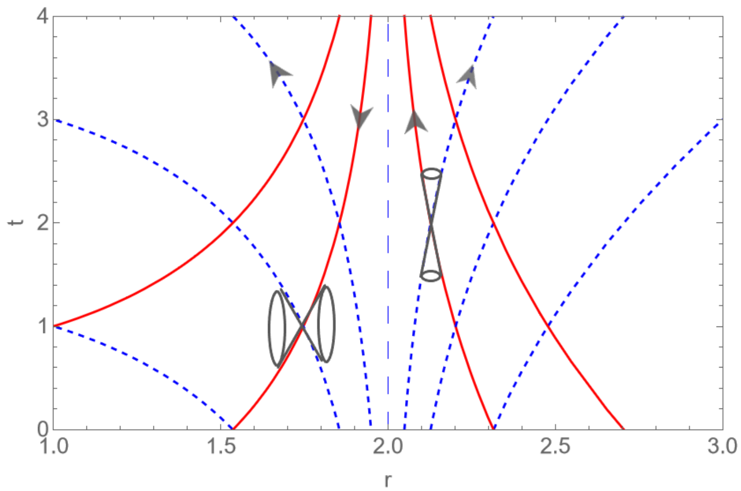

Figure 2.1: Null geodesics for Schwarzschild metric. The solid red lines corresponds to the ingoing lines whereas the dashed blue lines corresponds to the outgoing lines. The intersection between them define the light cones.

invariants defined above diverges at this point. As we are dealing with a vacuum solution, the Ricci and the Ricci squared vanish and the Kretschmann reads

$$R^{\mu\nu\rho\sigma}R_{\mu\nu\rho\sigma} = \frac{48M^2}{r^6} = \mathcal{K}. \tag{2.28}$$

Note that Eq. (2.28) reveals that $r = 0$ is the only real singularity of the solution so, the divergence of the metric at $r = R_S$ should correspond to a bad choice of coordinates. A more adequate set is given by the Eddington–Finkelstein coordiantes[23 24 25] which we define in what follows.

Let us consider the following transformation

$$\tilde{t} = t_\pm + 2M \ln |r - 2M|, \tag{2.29}$$

where $t_\pm$ is given by (2.24). Then, from (2.29) we get,

$$\tilde{t}_- = -r, \qquad \text{(ingoing)} \tag{2.30}$$

$$\tilde{t}_+ = r + 4M \ln |r - 2M|. \qquad \text{(outgoing)} \tag{2.31}$$

In figure 2.2 it is shown the spacetime diagram in the Eddintong–Finkelstein coordinates. Note that, the future world line that passes through the light cone goes form $r > 2M$ to $r < 2M$ which means that the particle can traverse the Schwarzschild radius in contrast to what is obtained in terms of the Schwarzschild coordinates. Furthermore, it is

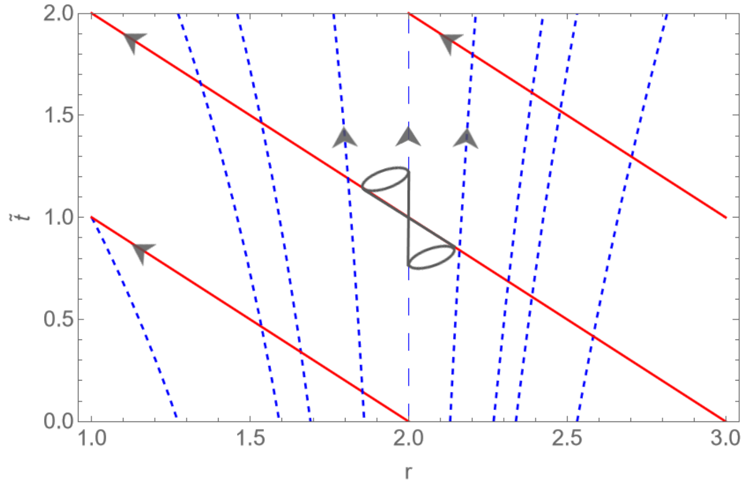

Figure 2.2: Null geodesics for Eddington–Finkelstein metric. The solid red lines corresponds to the ingoing lines whereas the dashed blue lines corresponds to the outgoing lines. The intersection between them define the light cones.

worth mentioning that once the particle traverse the event horizon, it will end up at $r = 0$ and moreover, the particle will not have a connection with the exterior region. In this respect, the regions $r < R_S$ and $r > R_S$ are causally disconnected and it is said that the surface $R_S = 2M$ defines the event horizon of the solution. Roughly speaking, the above configuration can be thought as the result of a complete gravitational collapse and, given that even light cannot escape from the $r < R_R$, it is known as Black Hole.

2.3 Schwarzschild interior solution

In this section we obtain the Schwarzschild interior configuration which corresponds to a static and spherically symmetric solution supported by a perfect fluid[26]. Let us parametrize the line element as

$$ds^2 = e^{\nu(r)}dt^2 - e^{\lambda(r)}dr^2 - r^2 d\Omega^2. \tag{2.32}$$

Using (2.32) and the energy momentum tensor for a perfect fluid given by Eq. (2.12), the Einstein field equations read[‡]

[‡]The intermediate steps are shown, in detail, in appendix A.

$$\kappa\rho = e^{-\lambda}\left(\frac{\lambda'}{r} - \frac{1}{r^2}\right) + \frac{1}{r^2}, \tag{2.33}$$

$$\kappa p = e^{-\lambda}\left(\frac{\nu'}{r} + \frac{1}{r^2}\right) - \frac{1}{r^2}, \tag{2.34}$$

$$\kappa p = \frac{e^{-\lambda}}{4}\left(2\nu'' + \nu'^2 + 2\frac{\nu'}{r} - \nu'\lambda' - 2\frac{\lambda'}{r}\right). \tag{2.35}$$

Note that Eqs. (B.3), (B.3) and (B.3) correspond to a set of three equations and four unknowns, namely $\{\nu, \lambda, \rho, p\}$, so an extra condition should be provided in order to close the system. In this case, we shall assume an uniform energy density, namely $\rho = \rho_0$, which is equivalent to

$$e^{-\lambda} = 1 - \frac{r^2}{C^2}, \tag{2.36}$$

from where

$$e^{\nu} = \left[A - B\left(1 - \frac{r^2}{C^2}\right)^{1/2}\right]^2. \tag{2.37}$$

Using (2.36) and (2.37), the matter sector reads

$$\kappa\rho = \frac{3}{C^2}, \tag{2.38}$$

or

$$\kappa p = \frac{1}{C^2}\left[\frac{3B(1 - r^2/C^2)^{1/2} - A}{A - B(1 - r^2/C^2)^{1/2}}\right]. \tag{2.39}$$

2.3.1 Matching conditions

The interior solution obtained previously contains indeterminacies encoded in the constant of integration. In order to provide a physical meaning of such constants, it is required to match the interior configuration with some exterior geometry at $r = R$ which defines the radius of the star. In this regard, a set of necessary and sufficient conditions are the continuity of the first and the second fundamental form which read

$$\left[ds^2\right]_\Sigma = 0, \tag{2.40}$$

and

$$\left[G_{\mu\nu}r^\nu\right]_\Sigma = 0, \tag{2.41}$$

where Σ corresponds to the surface of the star. Using (2.32), Eq. (2.40) reads $e^\nu|_{\Sigma^-} = e^\nu|_{\Sigma^+}$ and $e^\lambda|_{\Sigma^-} = e^\lambda|_{\Sigma^+}$. Now, if we consider the exterior Schwarzschild solution as the exterior geometry we obtain

$$e^{\nu(R)} = e^{-\lambda(R)} = 1 - \frac{2M}{R}, \tag{2.42}$$

with M and R the total mass and the radius of the star, respectively.

Similarly, the second fundamental form leads to $p|_{\Sigma^-} = p|_{\Sigma^+}$ which in this case reads

$$p(R) = 0. \tag{2.43}$$

For the Schwarzschild interior solution we have

$$C^2 = \frac{R^3}{2M}, \tag{2.44}$$

$$A = 3B\sqrt{1 - \frac{2M}{R}}, \tag{2.45}$$

$$B = 1/2. \tag{2.46}$$

Finally, the metric of the metric can be written as

$$ds^2 = \left[\frac{1}{4}\left(3\sqrt{1 - H^2R^2} - \sqrt{1 - H^2r^2}\right)^2\right]dt^2 - \left(1 - H^2r^2\right)^{-1}dr^2 - r^2\left(d\theta^2 + \sin\theta^2 d\phi^2\right), \tag{2.47}$$

where $H^2 = \frac{2M}{R^3}$.

The previous development represent one of the most important and simple interior solutions. However, there are different solutions as a consequence of the application of distinct assumptions according to the problem we want to solve (see Appendix B for instance).

2.4 Minimal Geometric Deformation

2.4.1 Einstein field equations by MGD

In this section we review some aspects of GD by MGD (for more details, see[27]). Let us start with the Einstein field equations (EFE)

$$G_{\mu\nu} = R_{\mu\nu} - \frac{1}{2}g_{\mu\nu}R = \kappa T_{\mu\nu} \tag{2.48}$$

where

$$T_{\mu\nu} = T^{(s)}_{\mu\nu} + \alpha\theta_{\mu\nu}\ . \tag{2.49}$$

In the above equation $\kappa = 8\pi$ represents the matter content of a known solution of Einstein's field equations, namely the *seed* sector, and $\theta_{\mu\nu}$ describes an extra source that is coupled by means of the parameter α. Such a coupling is introduced in order to control the effect of $\theta_{\mu\nu}$ on $T^{(s)}_{\mu\nu}$. Since the Einstein tensor satisfies the Bianchi identity [28], the total energy–momentum tensor satisfies

$$\nabla_\mu T^{\mu\nu} = 0 \ . \tag{2.50}$$

It is important to point out that, whenever $\nabla_\mu T^{\mu\nu(s)} = 0$, the following condition necessarily must be satisfied

$$\nabla_\mu \theta^{\mu\nu} = 0 \ , \tag{2.51}$$

and as a consequence, there is no exchange of energy-momentum tensor between the seed solution and the extra source $\theta^{\mu\nu}$ (the interaction is purely gravitational).

From now on, let us consider a static, spherically symmetric space-time sourced by

$$T^{\mu(s)}_\nu = \mathrm{diag}(\rho^{(s)}, -p^{(s)}_r, -p^{(s)}_\perp, -p^{(s)}_\perp) \tag{2.52}$$

$$\theta^\mu_\nu = \mathrm{diag}(\theta^0_0, \theta^1_1, \theta^2_2, \theta^2_2) \tag{2.53}$$

and a line element given by

$$ds^2 = e^\nu dt^2 - e^\lambda dr^2 - r^2(\theta^2 + \sin^2\theta d\phi^2). \tag{2.54}$$

Replacing (2.52), (2.53) and (2.54) in (2.1) and (2.49), the EFE read

$$\kappa\rho = \frac{1}{r^2} + e^{-\lambda}\left(\frac{\lambda'}{r} - \frac{1}{r^2}\right), \tag{2.55}$$

$$\kappa p_r = -\frac{1}{r^2} + e^{-\lambda}\left(\frac{\nu'}{r} + \frac{1}{r^2}\right), \tag{2.56}$$

$$\kappa p_\perp = \frac{1}{4}e^{-\lambda}\left(2\nu'' + \nu'^2 - \lambda'\nu' + 2\frac{\nu' - \lambda'}{r}\right) \tag{2.57}$$

where we have defined

$$\rho = \rho^{(s)} + \alpha\theta^0_0 \ , \tag{2.58}$$

$$p_r = p^{(s)}_r - \alpha\theta^1_1 \ , \tag{2.59}$$

$$p_\perp = p^{(s)}_\perp - \alpha\theta^2_2 \ . \tag{2.60}$$

Note that given the non-linearity of Einstein equations the decomposition (2.49) does not lead to two set of equations, one for each source involved. Nevertheless, contrary to the broadly belief, such a decoupling is possible in the context of MGD as we shall demonstrate in what follows.

2.4.2 Gravitational decoupling

Let us introduce a *geometric deformation* in the metric functions given by

$$\nu \longrightarrow \xi + \alpha g, \tag{2.61}$$

$$e^{-\lambda} \longrightarrow e^{-\mu} + \alpha f\ , \tag{2.62}$$

where $\{f, g\}$ are the so-called decoupling functions and α is the same free parameter that "controls" the influence of $\theta_{\mu\nu}$ on $T^{(s)}_{\mu\nu}$. In this work we shall concentrate in the particular case $g = 0$ and $f \neq 0$. Now, replacing (2.61) and (2.62) in the system (2.55-2.57), we are able to split the complete set of differential equations into two subsets: one describing a seed sector sourced by the conserved energy-momentum tensor, $T^{(s)}_{\mu\nu}$

$$\kappa\rho^{(s)} = \frac{1}{r^2} + e^{-\mu}\left(\frac{\mu'}{r} - \frac{1}{r^2}\right), \tag{2.63}$$

$$\kappa p_r^{(s)} = -\frac{1}{r^2} + e^{-\mu}\left(\frac{\nu'}{r} + \frac{1}{r^2}\right), \tag{2.64}$$

$$\kappa p_\perp^{(s)} = \frac{1}{4}e^{-\mu}\left(2\nu'' + \nu'^2 - \mu'\nu' + 2\frac{\nu' - \mu'}{r}\right), \tag{2.65}$$

and the other set corresponding to quasi-Einstein field equations sourced by $\theta_{\mu\nu}$

$$\kappa\theta_0^0 = -\frac{f}{r^2} - \frac{f'}{r}\ , \tag{2.66}$$

$$\kappa\theta_1^1 = -f\left(\frac{\nu'}{r} + \frac{1}{r^2}\right), \tag{2.67}$$

$$\kappa\theta_2^2 = -\frac{f}{4}\left(2\nu'' + \nu'^2 + 2\frac{\nu'}{r}\right) - \frac{f'}{4}\left(\nu' + \frac{2}{r}\right). \tag{2.68}$$

As we have seen, the components of $\theta_{\mu\nu}$ satisfy the conservation equation $\nabla_\mu\theta^\mu_\nu = 0$, namely

$$\theta_1'^1 - \frac{\nu'}{2}(\theta_0^0 - \theta_1^1) - \frac{2}{r}(\theta_2^2 - \theta_1^1) = 0. \tag{2.69}$$

Deformed vacuum

Hitherto, we have discussed the general aspects of GD by MGD without any specification of the system under study. However, if the system under consideration is the interior of some stellar configuration, the solution obtained will be valid only up to certain radius R which define the surface of the star. In this regard, the matching between the interior solution with some exterior geometry for $r > R$ is mandatory and in most of the cases, it is sufficient to take the Schwarzschild vacuum solution as the exterior metric. However, as it was demonstrated in [15], a suitable MGD–gravastar solution is possible whenever the exterior geometry is also a MGD–modified vacuum, namely

$$ds^2 = \left(1 - \frac{2M}{r}\right) dt^2 \quad - \quad \left[1 - \frac{2M}{r} + \alpha g(r)\right]^{-1} dr^2 - r^2 d\theta^2 - r^2 \sin^2\theta \, d\phi^2 \,, \tag{2.70}$$

with $g(r)$ is the decoupling function for the exterior solution. A list of MGD–modified vacuum solutions can be found in Ref. [29]. Now, in order to match smoothly the interior metric with the outside one above on the boundary surface Σ, we require

$$e^{\nu}\Big|_{\Sigma^-} = \left(1 - \frac{2M}{r}\right)\Big|_{\Sigma^+} , \tag{2.71}$$

$$e^{\lambda}\Big|_{\Sigma^-} = \left[1 - \frac{2M}{r} + \alpha g(r)\right]^{-1}\Bigg|_{\Sigma^+} , \tag{2.72}$$

$$p_r(r)\Big|_{\Sigma^-} = p_r(r)\Big|_{\Sigma^+} , \tag{2.73}$$

which corresponds to the continuity of the first and second fundamental form across that surface.

To conclude this section, we would like to emphasize the importance of GD by MGD as a useful tool to find solutions of EFE. As it is well known, in static and spherically symmetric spacetimes sourced by anisotropic fluids, EFE reduce to three equations given by (2.55), (2.56) and (2.57) and five unknowns, namely $\{\nu, \lambda, \rho, p_r, p_\perp\}$. In this sense, two auxiliary conditions must be provided: metric conditions, equations of state, etc. However, given that in the context of MGD a seed solution should be given, the number of degrees of freedom reduces to four and, as a consequence, only one extra condition is required. In general, this condition is implemented in the decoupling sector given by Eqs. (2.66), (2.67) and (2.68) as some equation of state which leads to a differential equation for the decoupling function f. In this work, we take an alternative route to find the decoupling function; namely, the complexity factor that we shall introduce in the next section.

2.5 Complexity of compact sources

Recently, a new definition for complexity for self–gravitating fluid distributions has been introduced in Ref. [16]. This definition is based on the intuitive idea that the least complex gravitational system should be characterized by a homogeneous energy density distribution and isotropic pressure. Now, as demonstrated in [16], there is a scalar associated to the orthogonal splitting of the Riemann tensor [30] in spherically symmetric space–times which capture the essence of what we mean by complexity, namely

$$Y_{TF} = 8\pi\Pi - \frac{4\pi}{r^3} \int_0^r \tilde{r}^3 \rho' d\tilde{r}, \tag{2.74}$$

with $\Pi \equiv p_r - p_\perp$. Also, it can be shown that (2.74) allows to write the Tolman mass as,

$$m_T = (m_T)_\Sigma \left(\frac{r}{r_\Sigma}\right)^3 + r^3 \int_r^{r_\Sigma} \frac{e^{(\nu+\lambda)/2}}{\tilde{r}} Y_{TF} d\tilde{r}, \tag{2.75}$$

which can be considered as a solid argument to define the complexity factor by means of this scalar given that this function, encompasses all the modifications produced by the energy density inhomogeneity and the anisotropy of the pressure on the active gravitational mass.

Note that the vanishing complexity condition ($Y_{TF} = 0$) can be satisfied not only in the simplest case of isotropic and homogeneus system but in all the cases where

$$\Pi = \frac{1}{2r^3} \int_0^r \tilde{r}^3 \rho' d\tilde{r}. \tag{2.76}$$

In this respect, the vanishing complexity condition leads to a non–local equation of state that can be used as a complementary condition to close the system of EFE (for a recent implementation, see [31], for example). Similarly, we can provide a particular values of Y_{TF} and use this information to find a family of solutions with the same complexity factor. An example of how this can be achieved can be found in [31]. In this work, we shall propose a suitable value for the complexity factor to find a new solution for an ultracompact star.

2.6 Ultracompact Schwarzschild star

In this section we briefly review the Schwarschild interior in the ultracompact regime. As it is well known, the metric for this configuration reads

$$ds^2 = e^\nu dt^2 - e^\lambda dr^2 - r^2 \left(d\theta^2 + \sin\theta^2 d\phi^2\right), \tag{2.77}$$

where

$$e^\nu = \frac{1}{4}\left(3\sqrt{1 - H^2R^2} - \sqrt{1 - H^2r^2}\right)^2 \tag{2.78}$$

$$e^{-\lambda} = 1 - H^2r^2, \tag{2.79}$$

with M the mass, R the radius of the star and

$$H^2 = \frac{2M}{R^3}. \tag{2.80}$$

The Schwarzschild interior is sourced by a perfect fluid with uniform density $\rho = \rho_0$ and a pressure given by

$$p = \rho_0 \left(\frac{1 - H^2 r^2 - \sqrt{1 - H^2 R^2}}{3\sqrt{1 - H^2 R^2} - \sqrt{1 - H^2 r^2}} \right). \tag{2.81}$$

At this point a couple of comments are in order. First, the Buchdahl limit set an upper bound of the compactness parameter, M/R, which entails a condition on the radius of the star, namely

$$R > \frac{9}{4} M > 2M. \tag{2.82}$$

The Buchdahl limit ensure that the pressure is finite and positive everywhere inside the star, as required for stable configurations. Second, note that the pressure (2.81) is regular except at some radius R_0 given by

$$R_0 = 3M \sqrt{1 - \frac{8}{9} \frac{R}{M}} < R. \tag{2.83}$$

Now, as noted by Mazur and Mottola, in the ultracompact limit, namely, when both R and R_0 approach to the Schwarzschild radius $2M$, the interior solution corresponds to a patch of the de Sitter solution. More precisely, the solution reads,

$$e^{\nu} = \frac{1}{4}\left(1 - H^2 r^2\right) \tag{2.84}$$

$$e^{-\lambda} = 1 - H^2 r^2 \tag{2.85}$$

$$p = -\rho = \text{constant}, \tag{2.86}$$

for $r < 2M$. It can be shown that the above solution join with the Schwarzschild vacuum in a way that the Israel second junction condition is violated. This implies that the presence of a δ–distribution of stresses is necessary to give a correct interpretation of the Schwarzschild star beyond the Buchdahl limit. However, as we shall demonstrate in what follows, the ultracompact solutions obtained by MGD does not require the existence of such a distribution of matter given that the metric functions join smoothly through the surface Σ.

Chapter 3

Results & Discussion

In this chapter, we develop a gravastar model supported by anisotropic fluids by the use of complexity.

3.1 Ultracompact star by gravitational decoupling

The MM gravastar given by (2.84), (2.85) and (2.86) was recently extended by MGD in [15]. In this case, the metric reads

$$
\begin{aligned}
e^{\nu} &= \frac{1}{4}\left(1 - H^2 r^2\right) \qquad (3.1)\\
e^{-\lambda} &= 1 - H^2 r^2 + \alpha f(r), \qquad (3.2)
\end{aligned}
$$

with

$$
f(r) = \left(1 - H^2 r^2\right) H^n r^n, \qquad (3.3)
$$

and $\alpha \geq -1$ to ensure that g^{rr} is positive definite as $r \to 2M$. As demonstrated in [15], the above solution is ill–matched with the Schwarzschild vacuum because it requires $\alpha = -3/2 < -1$ which violates the previous requirement for α to ensure the correct behaviour of g^{rr}. To overcome this difficulty, the proposed exterior solution was the modified vacuum

$$
\begin{aligned}
e^{\nu} &= = 1 - \frac{2M}{r} \qquad (3.4)\\
e^{-\lambda} &= \left(1 - \frac{2M}{r}\right)\left(1 + \frac{\ell}{2r - 3M}\right), \qquad (3.5)
\end{aligned}
$$

with ℓ a constant with units of a length. The reader is referred to Ref.[29] where the MGD–modified vacuum (3.4) and (3.5) was obtained and discussed in detail. It is worth mentioning that the decoupling function (3.3) leads to stable interior solutions only for $n = 2$.

The figure 3.1 we show the radial metric as a function of the radius. The function is non uniform and monotonic as expected. Besides, since it is positive everywhere, it indicates the absence of the Event Horizon.

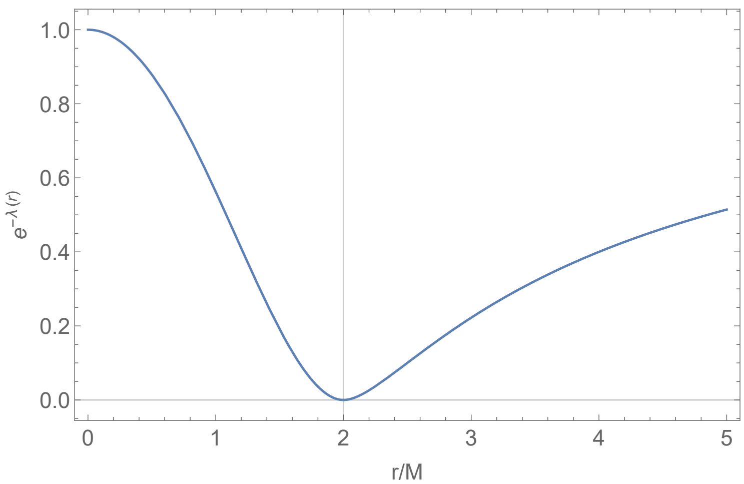

Figure 3.1: The deformed radial metric component for a gravastar $n = 2$ and $N = 2$.

The matter sector for this solution reads

$$\rho = \begin{cases} \frac{24M^2-5r^2}{(8\pi)16M^4} & r < 2, \\ \frac{M^2}{8\pi r^2(2r-3M)^2} & r > 2, \end{cases} \tag{3.6}$$

$$p_r = \begin{cases} \frac{3r^2}{(8\pi)16M^4} - \frac{1}{8\pi M^2} & r < 2, \\ -\frac{M}{8\pi r^2(2r-3M)} & r > 2, \end{cases} \tag{3.7}$$

$$p_\perp = \begin{cases} \frac{5r^2}{(8\pi)16M^4} - \frac{1}{8\pi M^2} & r < 2, \\ \frac{M(r-M)}{8\pi r^2(2r-3M)^2} & r > 2, \end{cases} \tag{3.8}$$

In figure 3.2 it is shown the density, the radial and the tangential pressure. Note that the density is monotonously decreasing as required and the tangential pressure has a discontinuity that remarks the surface of the star.

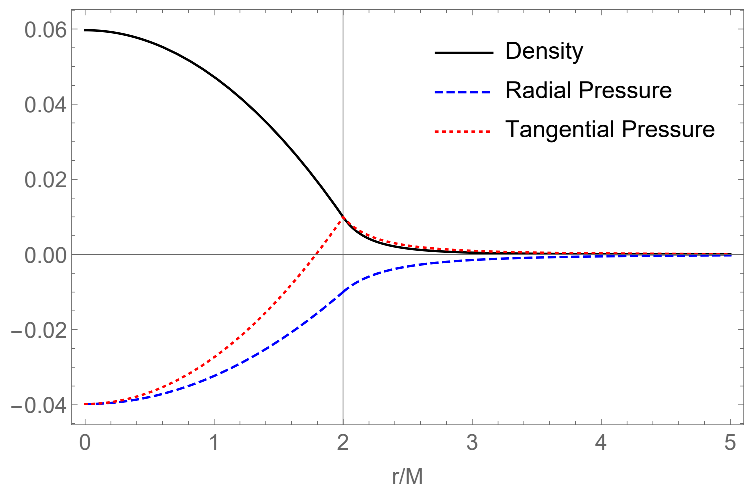

Figure 3.2: The density $\tilde{\rho}$ (black line), the radial pressure $\tilde{p}_r$ (dashed blue line) and the tangential pressure $\tilde{p}_t$ (dotted red line), with $\alpha = -1$ and $\ell = -M$, for a gravastar $n = 2$ and $N = 2$.

3.2 Ultracompact stars with polynomial complexity

In order to provide an alternative MGD–gravastar solution, in this work we use the complexity factor previously introduced in Sect. 2.5, as an auxiliary condition to close the system and find the decoupling function f. It can be checked that, imposing the broadly used vanishing complexity condition, it does not lead to well behaved interiors so in this work we shall provide another value for the complexity and we shall use the solution given by (3.1), (3.2) and (3.3) as a guide.

A straightforward computation reveals that for $n = 2$, the MGD gravastar model of Ref. [15] has a complexity given by

$$Y_{TF} = \alpha H^4 r^2. \tag{3.9}$$

Based on the above result, in this work we propose a polynomial complexity, namely

$$Y_{TF} = \sum_{i=0}^{N} a_i r^i, \tag{3.10}$$

which contains (3.9) as a particular case. Indeed, (3.9) is recovered for $N = 2$, $a_0 = a_1 = 0$ and $a_2 = \alpha H^4$. Now, replacing (3.1) and (3.2) in (3.10) we obtain

$$\frac{\alpha H^2 r\left[H^2 r\,(2f - rf') + f'\right]}{2\left(H^2 r^2 - 1\right)^2} = \sum_{i=0}^{N} a_i r^i, \tag{3.11}$$

which depending on the values of N, provides a differential equation for the decoupling function.

It can be shown that if either a_0 or a_1 are not vanishing factors, the solution of (3.11) leads to divergent interior solutions so this possibilities must be discarded and, as a consequence, (3.11) now reads

$$\frac{\alpha H^2 r\left[H^2 r\,(2f - rf') + f'\right]}{2\left(H^2 r^2 - 1\right)^2} = \sum_{i\geq 2}^{N} a_i r^i, \tag{3.12}$$

which can be easily integrated to obtain

$$f = -\frac{2}{\alpha H^2}\left(1 - H^2 r^2\right)\sum_{i\geq 2}^{N} \frac{a_i r^i}{i}. \tag{3.13}$$

For example, for $N = 3$ we obtain

$$f = \frac{2}{\alpha H^2}\left(1 - H^2 r^2\right)\left(\frac{a_2 r^2}{2} + \frac{a_3 r^3}{3}\right), \tag{3.14}$$

from where

$$e^{\nu} = \frac{1}{4}\left(1 - H^2 r^2\right), \tag{3.15}$$

$$e^{-\lambda} = \left(1 - H^2 r^2\right)\left[1 - \frac{2}{H^2}\left(\frac{a_2}{2} r^2 + \frac{a_3}{3} r^3\right)\right], \tag{3.16}$$

$$\rho = -\frac{9a_2 + 8a_3 r}{24\pi H^2} + \frac{15a_2 r^2 + 12a_3 r^3}{24\pi} + \frac{3H^2}{8\pi}, \tag{3.17}$$

$$p_r = \frac{3a_2 + 2a_3 r}{24\pi H^2} - \frac{9a_2 r^2 + 6a_3 r^3}{24\pi} - \frac{3H^2}{8\pi}, \tag{3.18}$$

$$p_\perp = \frac{a_2 + a_3 r}{8\pi H^2} - \frac{5a_2 r^2 + 4a_3 r^3}{8\pi} - \frac{3H^2}{8\pi}. \tag{3.19}$$

It is worth mentioning that in Eq. (3.14) we have discarded the term with the integration constant because it leads to divergence in the interior of the configuration.

To proceed with the analysis, we need to provide an exterior geometry and we shall explore two different MGD–modified vacuum.

3.2.1 Exterior 1

Let us consider

$$e^{\nu} = 1 - \frac{2M}{r}, \tag{3.20}$$

$$e^{-\lambda} = \left(1 - \frac{2M}{r}\right)\left(1 + \frac{\ell}{2r - 3M}\right), \tag{3.21}$$

$$\rho = -\frac{\ell M}{8\pi r^2 (3M - 2r)^2}, \tag{3.22}$$

$$p_r = -\frac{\ell}{24\pi M r^2 - 16\pi r^3}, \tag{3.23}$$

$$p_{\perp} = \frac{\ell(M - r)}{8\pi r^2 (3M - 2r)^2}. \tag{3.24}$$

The continuity of the radial pressure requires

$$a_2 = -\frac{128 a_3 M^6 + 3l + 9M}{96 M^5}, \tag{3.25}$$

while the continuity of the first fundamental form is automatically fulfilled.

In figure 3.3 we show how the radial metric $e^{-\lambda}$ as a function of r for the specific values in the legend.

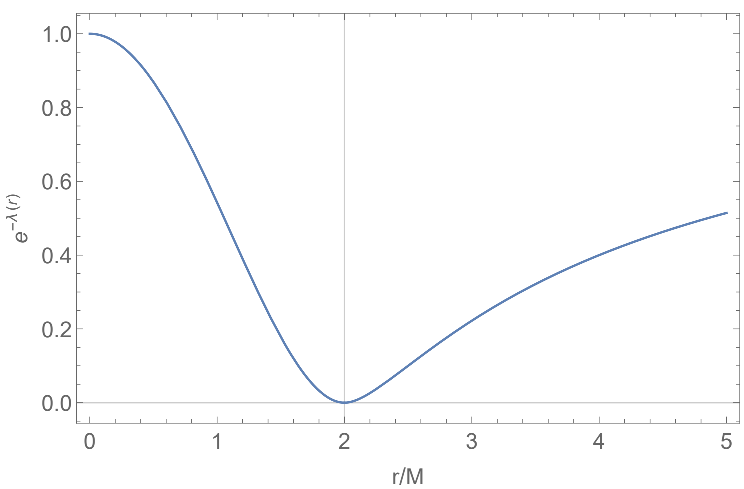

Figure 3.3: Deformed radial metric component of the first exterior geometry by polynomial complexity up to third order.

Note that, as in Ref.[15], the metric function $e^{-\lambda}$ is smoothly continuous though the stellar surface. In figure 3.4 we show the matter sector for the specific values in the legend where we note that not only the radial pressure but the density are continuous though the surface Σ in accordance with the results previously reported in[15]. In addition, note that the cusp–like matching of the tangential defines the surface of the star.

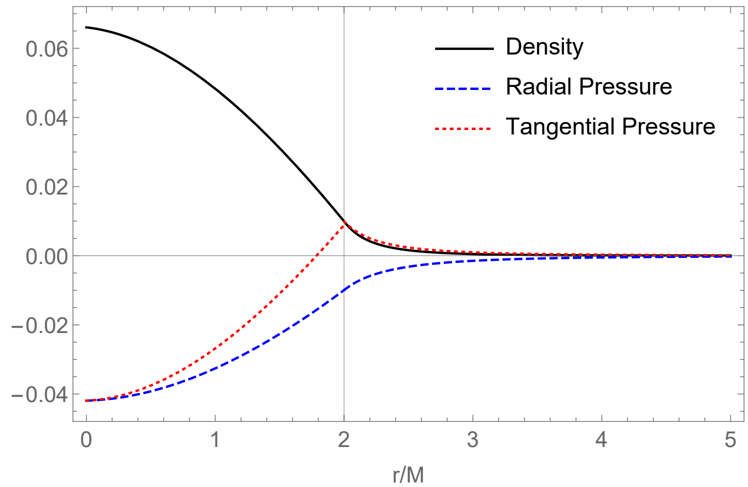

Figure 3.4: ρ (black line), p_r (blue dashed line) and $p_\perp$ (red dotted line) for $a_3 = 0.01$ and $l = -1$

3.2.2 Exterior 2

In this case we consider the MGD–deformed vacuum (see Ref.[29] for details)

$$e^{\nu} = 1 - \frac{2M}{r}, \tag{3.26}$$

$$e^{-\lambda} = \left(1 - \frac{2M}{r}\right)\left[1 + \frac{\beta}{(r+M)^{2(a-1)}}\right], \tag{3.27}$$

$$\rho = \frac{\beta\,(M+r)^{1-2a}\,[(3-4a)M + (2a-3)r]}{8\pi r^2}, \tag{3.28}$$

$$p_r = \frac{\beta(M+r)^{2-2a}}{8\pi r^2}, \tag{3.29}$$

$$p_\perp = \beta\frac{(a-1)(M-r)(M+r)^{1-2a}}{8\pi r^2}, \tag{3.30}$$

where $a > 1$ to ensure asymptotic flatness. The continuity of the radial pressure leads to

$$a_2 = -\frac{1}{32}3^{-2a-1}M^{-2a-4}\left(128\; 3^{2a}a_3M^{2a+5} + 3^{2a+2}M^{2a} + 27\beta M^2\right), \tag{3.31}$$

and, as in the previous case the continuity of the first fundamental form is satisfied by construction.

In figure 3.5 we show how the radial metric $e^{-\lambda}$ as a function of r for the specific values in the legend. Again, it is noticeable the smooth behaviour of the metric function.

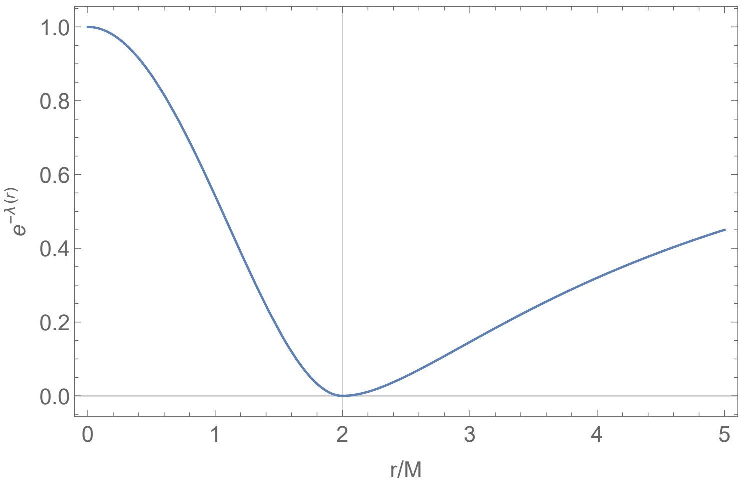

Figure 3.5: Deformed radial metric component of the second exterior geometry by polynomial complexity up to third order.

In figure 3.6 we show the matter sector as a function of r for the specific values in the legend and again, we note the continuity in both the radial pressure and the density. However, in contrast to the previous case, the tangential pressure is discontinuous at the surface.

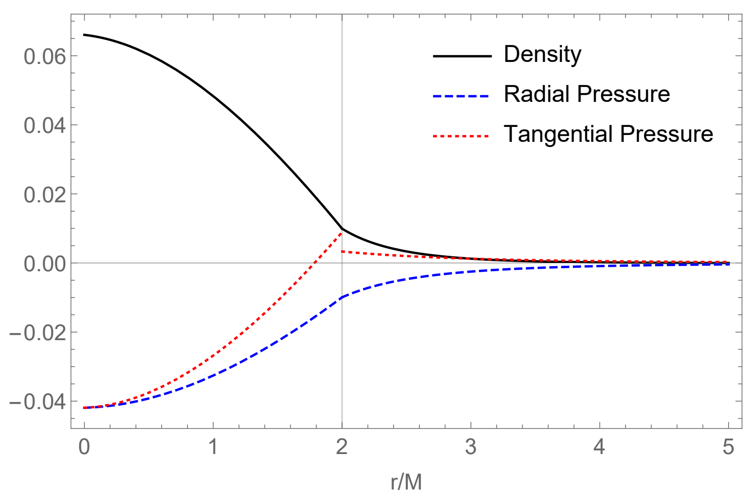

Figure 3.6: ρ (black line), p_r (blue dashed line) and $p_\perp$ (red dotted line) for $a_3 = 0.01, \beta = -9$ and $a = 2$

Chapter 4

Conclusions & Outlook

In this work we constructed a new ultracompact anisotropic star solution in the framework of the Gravitational Decoupling by the Minimal Geometric Deformation approach. As the auxiliary condition to close the system of differential equations we used the complexity factor of self–gravitating fluids. Inspired by the results found in [15], we proposed a polynomial complexity and obtained that the interior solution obtain can be well–matched to two different modified vacuum. The solution obtained here, contains the reported in Ref. [15] as an special case. Ore findings here indicate that the solution fulfill the requirements of a stable configuration, namely, i) the solution is regular at the origin, ii) the mass and the radius are well defined, iii) the density is positive everywhere and decreases monotonically to the surface and iv) the radial pressure is non–uniform and monotonic as expected.

Although we only analysed the case $N = 3$ here, it can be easily shown that higher orders can also provide suitable gravastar models for particular values of the free parameters involved (see for instance, appendix C). However, it should be interesting to consider higher orders in the polynomial complexity matched to different modified vacuum to explore to what extend the model leads to well behaved solutions.

Appendix A

Interior Schwarzschild solution

Given the metric,

$$ds^2 = e^{\nu(r)}dt^2 - e^{-\lambda(r)}dr^2 - r^2 d\Omega^2,$$

we can calculate the Christoffel symbols using equation,

$$\Gamma^{\nu}_{\lambda\mu} = \frac{1}{2}g^{\nu\sigma}(\partial_\mu g_{\sigma\lambda} + \partial_\lambda g_{\sigma\mu} - \partial_\sigma g_{\mu\lambda}).$$

Note that, here we are going to represent the derivative with a simple comma (,). Moreover, in the calculation we can note that in all the cases, most of the components will vanish or will cancel due to the diagonalization of the metric. Then, the nonzero Christoffel symbols are,

$$\begin{aligned}\Gamma^0_{01} &= \frac{1}{2}g^{00}\left(g_{00,1} + \cancel{g_{01,0}} - \cancel{g_{01,0}}\right),\\ &= \frac{1}{2}\frac{1}{e^\nu}\frac{\partial}{\partial r}e^\nu = \frac{\nu'}{2},\end{aligned} \tag{A.1}$$

$$\begin{aligned}\Gamma^1_{00} &= \frac{1}{2}g^{11}\left(\cancel{g_{10,0}} + \cancel{g_{10,0}} - g_{00,1}\right),\\ &= \frac{1}{2}\left(-\frac{1}{e^\lambda}\right)\left(-\frac{\partial}{\partial r}e^\nu\right) = \frac{\nu'}{2}e^{-\lambda+\nu},\end{aligned} \tag{A.2}$$

$$\begin{aligned}\Gamma^1_{11} &= \frac{1}{2}g^{11}\left(g_{10,0} + \cancel{g_{10,0}} - \cancel{g_{00,1}}\right),\\ &= \frac{1}{2}\left(-\frac{1}{e^\lambda}\right)\left(-\frac{\partial}{\partial r}e^\lambda\right) = \frac{\lambda'}{2},\end{aligned} \tag{A.3}$$

$$\begin{aligned}\Gamma^1_{22} =& \frac{1}{2} g^{11} \left(\cancel{g_{12,2}} + \cancel{g_{12,2}} - g_{22,1} \right), \\ =& \frac{1}{2}\left(-\frac{1}{e^\lambda}\right)\left(-\frac{\partial}{\partial r} r^2\right) = -re^{-\lambda},\end{aligned} \tag{A.4}$$

$$\begin{aligned}\Gamma^1_{33} =& \frac{1}{2} g^{11} \left(\cancel{g_{13,3}} + \cancel{g_{13,3}} - g_{33,1} \right), \\ =& \frac{1}{2}\left(-\frac{1}{e^\lambda}\right)\left[-\frac{\partial}{\partial r} r^2 \sin^2(\theta)\right], \\ =& - r\sin^2(\theta) e^{-\lambda},\end{aligned} \tag{A.5}$$

$$\begin{aligned}\Gamma^2_{12} =& \frac{1}{2} g^{22} \left(\cancel{g_{21,2}} + g_{22,1} - \cancel{g_{12,2}} \right), \\ =& \frac{1}{2}\left(-\frac{1}{r^2}\right)\left(-\frac{\partial}{\partial r} r^2\right) = \frac{1}{r},\end{aligned} \tag{A.6}$$

$$\begin{aligned}\Gamma^2_{33} =& \frac{1}{2} g^{22} \left(\cancel{g_{23,3}} + \cancel{g_{23,3}} - g_{33,2} \right), \\ =& \frac{1}{2}\left(-\frac{1}{r^2}\right)\left[-\frac{\partial}{\partial \theta} r^2 \sin^2(\theta)\right], \\ =& - \sin(\theta)\cos(\theta),\end{aligned} \tag{A.7}$$

$$\begin{aligned}\Gamma^3_{13} =& \frac{1}{2} g^{33} \left(\cancel{g_{31,3}} + g_{33,1} - \cancel{g_{13,3}} \right), \\ =& \frac{1}{2}\left[-\frac{1}{r^2\sin^2(\theta)}\right]\left[-\frac{\partial}{\partial r} r^2 \sin^2(\theta)\right], \\ =& \frac{1}{r},\end{aligned} \tag{A.8}$$

$$\begin{aligned}\Gamma^3_{23} =& \frac{1}{2} g^{33} \left(\cancel{g_{32,3}} + g_{33,2} - \cancel{g_{23,3}} \right), \\ =& \frac{1}{2}\left[-\frac{1}{r^2\sin^2(\theta)}\right]\left[-\frac{\partial}{\partial \theta} r^2 \sin^2(\theta)\right], \\ =& \cot(\theta).\end{aligned} \tag{A.9}$$

Given the Christoffel symbols we can go through the Riemann tensor,

$$R^\lambda_{\mu\rho\nu} = \partial_\rho \Gamma^\lambda_{\mu\nu} - \partial_\nu \Gamma^\lambda_{\mu\rho} + \Gamma^\lambda_{\sigma\rho}\Gamma^\sigma_{\mu\nu} - \Gamma^\lambda_{\sigma\nu}\Gamma^\sigma_{\mu\rho}.$$

Then,

$$
\begin{aligned}
R^1_{010} &= \frac{e^{-\lambda+\nu}}{4}\left(\nu'^2 - \lambda'\nu' + 2\nu''\right), && \text{(A.10)}\\
R^2_{020} &= \frac{1}{r}\frac{\nu'}{2}e^{-\lambda+\nu}, && \text{(A.11)}\\
R^3_{030} &= \frac{1}{r}\frac{\nu'}{2}e^{-\lambda+\nu}, && \text{(A.12)}\\
R^0_{101} &= \left(-\frac{\partial}{\partial r}\frac{\nu'}{2}\right) + \frac{\nu'}{2}\left(\frac{-\lambda}{2} - \frac{\nu'}{2}\right), && \text{(A.13)}\\
R^2_{121} &= \frac{\lambda'}{2r}, && \text{(A.14)}\\
R^3_{131} &= \frac{\lambda'}{2r}, && \text{(A.15)}\\
R^0_{202} &= \frac{\nu'}{2}\left(-re^{-\lambda}\right), && \text{(A.16)}\\
R^1_{212} &= \frac{\lambda'}{2}re^{-\lambda}, && \text{(A.17)}\\
R^3_{232} &= 1 - e^{-\lambda}, && \text{(A.18)}\\
R^0_{303} &= \frac{\nu'}{2}\left[-r\sin^2(\theta)e^{-\lambda}\right], && \text{(A.19)}\\
R^1_{313} &= \frac{\lambda'}{2}\left[-r\sin^2(\theta)e^{-\lambda}\right], && \text{(A.20)}\\
R^2_{323} &= \sin^2(\theta)\left(1 - e^{-\lambda}\right). && \text{(A.21)}
\end{aligned}
$$

Now, is possible for us to construct the Ricci tensor and the Ricci scalar,

$$
\begin{aligned}
R_{\mu\nu} &= R^{\alpha}_{\mu\alpha\nu},\\
R &= g^{\mu\nu}R_{\mu\nu},
\end{aligned}
$$

$$
\begin{aligned}
R_{00} &= \frac{e^{-\lambda+\nu}}{4r}\left[\nu'(4 - \lambda' r) + r\nu'^2 + 2\nu'' r\right], && \text{(A.22)}\\
R_{11} &= \frac{1}{4r}\left[\lambda'(4 + r\nu') - r\nu'^2 - 2r\nu''\right], && \text{(A.23)}\\
R_{22} &= \frac{e^{-\lambda}}{2}\left(r\lambda' - r\nu' + 2e^{\lambda} - 2\right), && \text{(A.24)}\\
R_{33} &= \frac{e^{-\lambda}}{2}\sin^2(\theta)\left(r\lambda' - r\nu' + 2e^{\lambda} - 2\right), && \text{(A.25)}
\end{aligned}
$$

and,

$$
R = \frac{e^{-\lambda}}{2r^2}\left(4r\nu' - 4r\lambda' + r^2\nu'^2 + 2r^2\nu'' - 4e^{\lambda} + 4 - r^2\nu'\lambda'\right). \tag{A.26}
$$

Then, we can compose the Einstein tensor $G_{\mu\nu}$,

$$G_{\mu\nu} = R_{\mu\nu} - \frac{1}{2} g_{\mu\nu} R = kT_{\mu\nu}.$$

Therefore, we have,

$$G_0^0 = \frac{1}{r^2}\left[r\left(1 - e^{-\lambda}\right)\right]' = k\rho, \tag{A.27}$$

$$G_1^1 = -\frac{1}{r^2}\left(1 - e^{-\lambda}\right) + \frac{\nu'}{r} e^{-\lambda} = kp, \tag{A.28}$$

$$G_2^2 = \frac{e^{-\lambda}}{4}\left(2\nu'' + \nu'^2 + 2\frac{\nu'}{r} - \nu'\lambda' - 2\frac{\lambda'}{r}\right) = kp, \tag{A.29}$$

where the last equation can be rewritten as,

$$0 = \frac{\mathbf{d}}{\mathbf{d}r}\left(\frac{e^{-\lambda} - 1}{r^2}\right) + \frac{\mathbf{d}}{\mathbf{d}r}\left(\frac{e^{-\lambda}\nu'}{2r}\right) + e^{-\lambda-\nu}\frac{\mathbf{d}}{\mathbf{d}r}\left(\frac{e^{-\nu}\nu'}{2r}\right).$$

This change was made in order to make easier the calculation. Now, to solve Einstein equations we need to provide an extra information,

$$e^{-\lambda} = 1 - \frac{r^2}{C^2}.$$

Then, by the use of the previous equation we can simplify the Einstein equation for G_2^2,

$$\frac{\mathbf{d}}{\mathbf{d}r}\left[\left(1 - \frac{r^2}{C^2}\right)\frac{\nu'}{2r}\right] + \left(1 - \frac{r^2}{C^2}\right) e^{-\nu}\frac{\mathbf{d}}{\mathbf{d}r}\left(\frac{e^{-\nu}\nu'}{2r}\right) = 0, \tag{A.30}$$

After the derivation of the previous equation, we get a second order differential equation, all in terms of ν,

$$0 = \nu''\left(\frac{1}{r} - \frac{r}{C^2}\right) - \frac{\nu'}{r^2} + \frac{\nu'^2}{2}\left(\frac{1}{r} - \frac{r}{C^2}\right). \tag{A.31}$$

The previous equation (A.31) can be solved by using different mathematical methods, which results in,

$$e^{\nu} = \left[A - B\left(1 - \frac{r^2}{C^2}\right)^{1/2}\right]^2. \tag{A.32}$$

Finally, by using the previous solution we can solve easily the other Einstein field equations that after all, should be matched with the exterior solution by the use of the fundamental forms of continuity as was shown in the section 2.3.

Appendix B

Tolman IV solution

We are going to develop the *Tolman IV solution*[32]. We are dealing with a sphere of perfect fluid surrounded by vacuum. Then, in this case, we are going to solve EFE (B.3-B.3) making the following geometrical constrain,

$$\frac{e^{\nu}\nu'}{2r} = constant. \tag{B.1}$$

As we should note, the equation (B.1) is a simple differential equation, which can be solved in order to obtain a valid solution for $\nu(r)$. Then,

$$\begin{aligned}
\nu' &= \frac{B^2}{A^2} r e^{-\nu}, \\
\Rightarrow \nu &= \log\left(\frac{B^2}{A^2} r^2 + B^2\right),
\end{aligned}$$

from where

$$\Rightarrow e^{\nu} = B^2\left(1 + \frac{r^2}{A^2}\right). \tag{B.2}$$

The EFE reads,

$$\begin{aligned}
\kappa\rho &= e^{-\lambda}\left(\frac{\lambda'}{r} - \frac{1}{r^2}\right) + \frac{1}{r^2}, \\
\kappa p &= e^{-\lambda}\left(\frac{\nu'}{r} + \frac{1}{r^2}\right) - \frac{1}{r^2}, \\
\kappa p &= \frac{e^{-\lambda}}{4}\left(2\nu'' + \nu'^2 + 2\frac{\nu'}{r} - \nu'\lambda' - 2\frac{\lambda'}{r}\right),
\end{aligned}$$

where the last equation can be written in a more convenient way as[32]

$$0 = \frac{\mathbf{d}}{\mathbf{d}r}\left(\frac{e^{-\lambda} - 1}{r^2}\right) + \frac{\mathbf{d}}{\mathbf{d}r}\left(\frac{e^{-\lambda}\nu'}{2r}\right) + e^{-\lambda-\nu}\frac{\mathbf{d}}{\mathbf{d}r}\left(\frac{e^{-\nu}\nu'}{2r}\right).$$

Note that, the previous equation is simpler, because the first term vanishes due to the geometrical constrain. So that, making a simple integration we obtain,

$$\frac{e^{-\lambda} - 1}{r^2} + \frac{e^{-\lambda}\nu'}{2r} = -\frac{1}{C^2}. \tag{B.3}$$

As we can see in the above equation, $-\frac{1}{C^2}$ represents a simple constant as a consequence of the integration. Now, the second step is to substitute the solution of ν (B.2) into the previous equation. Then, at the end, we are going to have,

$$e^{-\lambda} = \frac{\left(1 - r^2/C^2\right)\left(1 + r^2/A^2\right)}{1 + 2r^2/A^2}. \tag{B.4}$$

With the previous solutions of ν and λ we obtain the expressions for the density and the pressure from the Einstein field equations, (B.3) and (B.3). Then, we have,

$$\kappa\rho = \frac{1}{A^2}\frac{1 + 3A^2/C^2 + 3r^2/C^2}{1 + 2r^2/A^2} + \frac{2}{A^2}\frac{1 - r^2/C^2}{(1 + 2r^2/A^2)^2},, \tag{B.5}$$

$$\kappa p = \frac{1}{A^2}\frac{1 - A^2/C^2 - 3r^2/C^2}{1 + 2r^2/A^2}. \tag{B.6}$$

Next, we need to apply the matching conditions in order to match the interior with the exterior solution for a smooth transition between these two. Then, the firs and second fundamental form of continuity (2.40 and 2.41) gives us the following values for the constants,

$$A^2 = \frac{R^2\,(R - 3M)}{M}, \tag{B.7}$$

$$B^2 = 1 - \frac{3M}{R}, \tag{B.8}$$

$$C^2 = \frac{R^3}{M}. \tag{B.9}$$

Then, the expressions for ν, λ, ρ and p are,

$$
\begin{aligned}
e^{\nu} &= 1+\frac{M\left(r^2-3R^2\right)}{R^3}, && \text{(B.10)}\\
e^{-\lambda} &= \frac{\left(R^3-Mr^2\right)\left[R^3+M\left(r^2-3R^2\right)\right]}{2MR^3r^2-3MR^5+R^6}, && \text{(B.11)}\\
\kappa\rho &= \frac{3M\left[2R^6+3MR^3\left(r^2-3R^2\right)+M^2\left(2r^4-7R^2r^2+9R^4\right)\right]}{R^3\left(2Mr^2-3MR^2+R^3\right)^2}, && \text{(B.12)}\\
\kappa p &= \frac{3M^2(R^2-r^2)}{2MR^3r^2-3MR^5+R^6}. && \text{(B.13)}
\end{aligned}
$$

With this in mind, we can actually see better the behavior of the density and the pressure inside the sphere of the perfect fluid. Figures (B.1) and (B.2) show the density function and the pressure function respectively. Actually, both functions took the values for the compactness parameter as 0.2 (i.e $u = M/R$). Moreover, the figures exhibit a decreasing behavior as was expected with the zero value in the region of $r = 2M$. Therefore, the interior solution was matched very good with the exterior vacuum configuration where the density and the pressure have a smooth transition to a constant zero value.

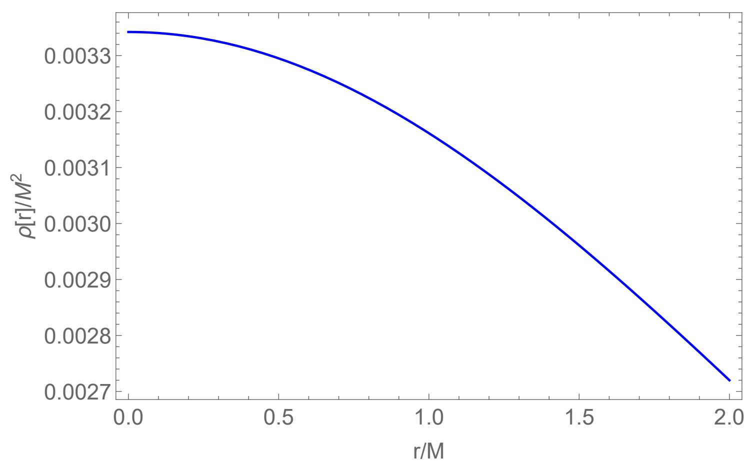

Figure B.1: Density function for Tolman IV solution with the compactness parameter of 0.2

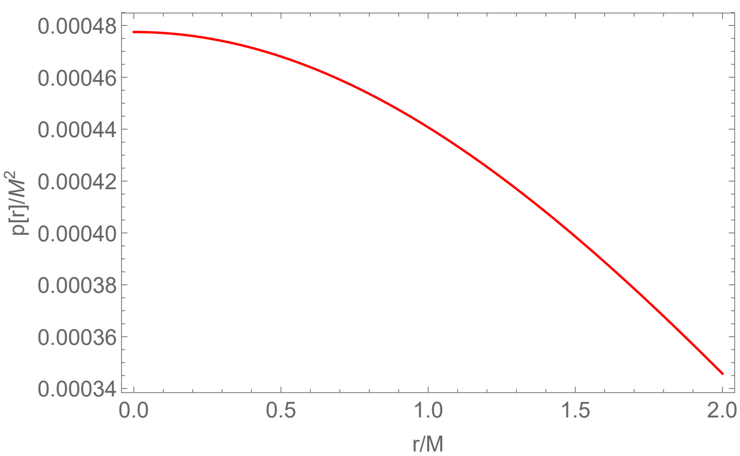

Figure B.2: Pressure function for Tolman IV solution with the compactness parameter of 0.2

Appendix C

Higher order solution for gravastar

The interior region of the gravastar by polynomial expression can be seen as,

$$f^* = \frac{2}{\alpha H^2}(1 - H^2 r^2) \sum_{i \geq 2}^{N} \frac{a_i r^i}{i}, \tag{C.1}$$

since in section 3.1 was devoted to the study of $N = 3$, we can consider a further case. Therefore, here we will treat the problem up to the fifth order. Again, we should notice that a_0 and a_1 must be zero in order to avoid singularities. With this in mind, our new interior function $f^*(r)$ has the form,

$$f^* = \frac{2}{\alpha H^2}(1 - H^2 r^2)\left(\frac{a_2}{2} r^2 + \frac{a_3 r^3}{3} + \frac{a_4 r^4}{4} + \frac{a_5 r^5}{5}\right), \tag{C.2}$$

with the previous expression, the metric components lead to,

$$e^{\nu} = \frac{1}{4}\left(1 - H^2 r^2\right), \tag{C.3}$$

$$e^{-\lambda} = \left(1 - H^2 r^2\right)\left[1 + \frac{2}{H^2}\left(\frac{a_2 r^2}{2} + \frac{a_3}{3} r^3 + \frac{a_4 r^4}{4} + \frac{a_5 r^5}{5}\right)\right]. \tag{C.4}$$

Then, the matter sector for $r < 2M$ read,

$$\rho = \frac{3H^2 r^3 \left[r\left(32 a_5 r + 35 a_4\right) + 40 a_3\right] + 30 a_2 \left(5H^2 r^2 - 3\right) - r\left(72 a_5 r^2 + 75 a_4 r + 80 a_3\right) + 90 H^4}{240 \pi H^2}, \tag{C.5}$$

$$p_r = \frac{-3H^2 r^3 \left[3r\left(4 a_5 r + 5 a_4\right) + 20 a_3\right] + a_2 \left(30 - 90 H^2 r^2\right) + r\left[3r\left(4 a_5 r + 5 a_4\right) + 20 a_3\right] - 90 H^4}{240 \pi H^2}, \tag{C.6}$$

$$p_{\perp} = \frac{-H^2 r^3 \left[r\left(32 a_5 r + 35 a_4\right) + 40 a_3\right] + a_2 \left(10 - 50 H^2 r^2\right) + 10 r\left[r\left(a_5 r + a_4\right) + a_3\right] - 30 H^4}{80 \pi H^2}. \tag{C.7}$$

while for the region $r > 2M$, we have

$$
\begin{aligned}
e^{\nu} &= 1 - \frac{2M}{r}, && \text{(C.8)}\\
e^{-\lambda} &= \left(1 - \frac{2M}{r}\right)\left(1 + \frac{\ell}{2r - 3M}\right), && \text{(C.9)}\\
\rho &= -\frac{\ell M}{8\pi r^2 (3M - 2r)^2}, && \text{(C.10)}\\
p_r &= -\frac{\ell}{24\pi M r^2 - 16\pi r^3}, && \text{(C.11)}\\
p_\perp &= \frac{\ell (M - r)}{8\pi r^2 (3M - 2r)^2}, && \text{(C.12)}
\end{aligned}
$$

likewise the section 3.2.1, the first fundamental form is automatically fulfilled and the continuity in the radial pressure gives us,

$$
a_2 = -\frac{1536 a_5 M^8 + 960 a_4 M^7 + 640 a_3 M^6 + 45M + 15\ell}{480 M^5}. \tag{C.13}
$$

As we see, since we increase the order in the polynomial complexity factor, we will have more and more degrees of freedom. In this particular case, for $N = 5$, we have 3 degrees of freedom. However, we should notice that for these unknown constants we have a condition in order to have a suitable model for our gravastar. This condition relates to the requirement that the deformed radial metric component should be positive with just one root at the surface of the star. Also, we should consider the decreasing behavior in the energy density function. Therefore, with these limitations, we should set all the values of the constants very small. For instance, in this case, we chose $a_3 = a_4 = a_5 = 0.001$ and $\ell = -M$ likewise the previous case for $N = 3$.

With this in mind, on the one hand the figure C.1 shows the effective parameters functions through the surface of the star at $r = 2M$. As we notice, they obey all the requirements to have a physically acceptable model. The density function decreases monotonically since we reach the surface. Moreover, the radial pressure and the density have smooth transitions between the interior and the exterior region. Whereas, the tangential pressure has no analytical solution at $r = 2M$.

On the other hand, The radial deformed metric component is illustrated in the figure C.2. The function is positive everywhere and it presents one root at exactly the surface of the star. As it was expected, we do not have an emergence of an event horizon since $e^{\lambda(r)}$ does not change its sign.

Furthermore, it can be shown that for the second exterior deformed function, we get a suitable solution too. Besides, we can consider cases of higher order terms which will give us well behaved solutions. However, while we increase the order, we will be increasing the unknown constants which give us some kind of limitation.

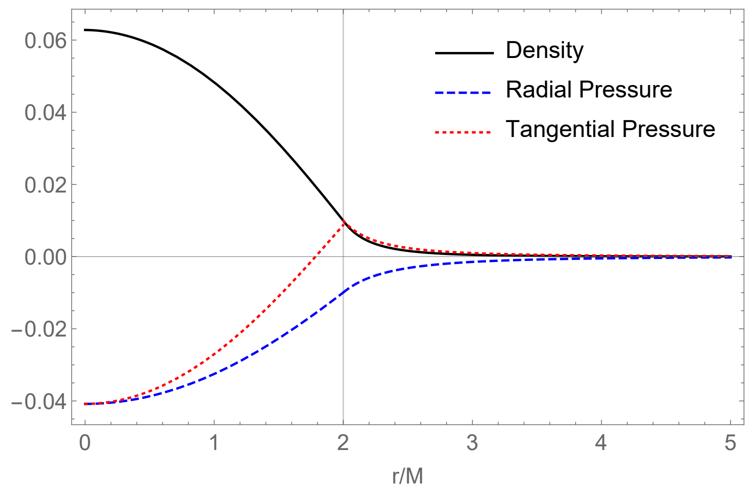

Figure C.1: Effective parameters for gravastar by complexity at the order of 5. The density ρ (black line), the radial pressure p_r (dashed blue line) and the tangential pressure $p_\perp$ (dotted red line) in the interior and in the exterior region of the ultracompact star, with $a_3 = a_4 = a_5 = 0.001$ and $\ell = -M$.

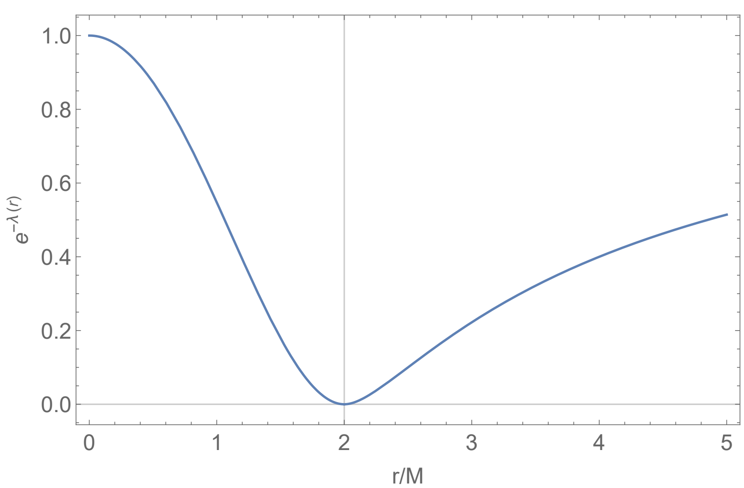

Figure C.2: Deformed radial metric component by complexity at N=5. The thick grey lines denote the surface of the star and the 0 limit to remark that the function is continuous and positive through the radius of the ultracompact star.

Bibliography

[1] Einstein, A. Die Feldgleichungen der Gravitation. *Sitzungsberichte der Königlich Preußischen Akademie der Wissenschaften (Berlin), Seite 844-847.* **1915**,

[2] Abbott, B. P. *et al.* Tests of General Relativity with GW150914. *Phys. Rev. Lett.* **2016**, *116*, 221101.

[3] Abbott, B. P. *et al.* GW170104: Observation of a 50-Solar-Mass Binary Black Hole Coalescence at Redshift 0.2. *Phys. Rev. Lett.* **2017**, *118*, 221101.

[4] Lee, H. M. Long Journey toward the Detection of Gravitational Waves and New Era of Gravitational Wave Astrophysics. *Journal of the Korean Physical Society* **2018**, *73*, 684–700.

[5] Akiyama, K.; Bouman, K.; Woody, D. First M87 Event Horizon Telescope Results. I. The Shadow of the Supermassive Black Hole. *Astrophysical Journal Letters* **2019**, *875*.

[6] others,, *et al.* First M87 event horizon telescope results. IV. Imaging the central supermassive black hole. *The Astrophysical Journal Letters* **2019**, *875*, L4.

[7] Bonanno, A.; Khosravi, A.-P.; Saueressig, F. Regular black holes with stable cores. *Phys. Rev. D* **2021**, *103*, 124027.

[8] Bargueño, P. Some global, analytical, and topological properties of regular black holes. *Physical Review D* **2020**, *102*.

[9] Dymnikova, I. Regular black holes and self-gravitating solitons with DE interiors. *International Journal of Modern Physics A* **2020**, *35*, 2040053.

[10] Konoplya, R. A.; Zhidenko, A. Traversable wormholes in General Relativity without exotic matter. 2021.

[11] Potashov, I.; Tchemarina, J.; Tsirulev, A. Null and Timelike Geodesics near the Throats of Phantom Scalar Field Wormholes. *Universe* **2020**, *6*, 183.

[12] Raposo, G.; Pani, P.; Bezares, M.; Palenzuela, C.; Cardoso, V. Anisotropic stars as ultracompact objects in general relativity. *Phys. Rev. D* **2019**, *99*, 104072.

[13] Mazur, P. O.; Mottola, E. Gravitational vacuum condensate stars. *Proceedings of the National Academy of Sciences* **2004**, *101*, 9545–9550.

[14] Raposo, G.; Pani, P.; Bezares, M.; Palenzuela, C.; Cardoso, V. Anisotropic stars as ultracompact objects in general relativity. *Phys. Rev. D* **2019**, *99*, 104072.

[15] Ovalle, J.; Posada, C.; Stuchlík, Z. Anisotropic ultracompact Schwarzschild star by gravitational decoupling. *Classical and Quantum Gravity* **2019**, *36*, 205010.

[16] Herrera, L. New definition of complexity for self-gravitating fluid distributions: The spherically symmetric, static case. *Physical Review D* **2018**, *97*, 044010.

[17] Carroll, S. M. *Spacetime and Geometry*; Cambridge University Press, 2004.

[18] D'Inverno, R.; D'Inverno, L. *Introducing Einstein's Relativity*; Comparative Pathobiology - Studies in the Postmodern Theory of Education; Clarendon Press, 1992.

[19] Misner, C. W.; Thorne, K. S.; Wheeler, J. A. In *San Francisco: W.H. Freeman and Co., 1973*; Misner, C. W., Thorne, K. S., & Wheeler, J. A.,, Ed.; 1973.

[20] Zee, A. *Einstein Gravity in a Nutshell*; In a Nutshell; Princeton University Press, 2013.

[21] Schutz, B. *A First Course in General Relativity*, 2nd ed.; Cambridge University Press, 2009.

[22] Schwarzschild, K. Über das Gravitationsfeld eines Massenpunktes nach der Einsteinschen Theorie. *Sitzungsberichte der Königlich Preußischen Akademie der Wissenschaften (Berlin)* **1916**, 189–196.

[23] Eddington, A. S. *The mathematical theory of relativity*; The University Press, 1923.

[24] Eddington, A. S. *Space, time and gravitation: An outline of the general relativity theory*; University Press, 1920.

[25] Finkelstein, D. Past-Future Asymmetry of the Gravitational Field of a Point Particle. *Phys. Rev.* **1958**, *110*, 965–967.

[26] Schwarzschild, K. Über das Gravitationsfeld einer Kugel aus inkompressibler Flüssigkeit nach der Einsteinschen Theorie. **1916**, 424–434.

[27] Ovalle, J. Decoupling gravitational sources in general relativity: From perfect to anisotropic fluids. *Physical Review D* **2017**, *95*.

[28] Bianchi, L. Sui simboli a quattro indici e sulla curvatura di Riemann. *Rend. Acc. Naz. Lincei* **1902**, *11*, 3–7.

[29] Ovalle, J.; Casadio, R.; da Rocha, R.; Sotomayor, A.; Stuchlík, Z. Black holes by gravitational decoupling. *The European Physical Journal C* **2018**, *78*, 1–11.

[30] Gómez-Lobo, A. G.-P. Dynamical laws of superenergy in general relativity. *Classical and Quantum Gravity* **2007**, *25*, 015006.

[31] Casadio, R.,; Contreras, E.,; Ovalle, J.,; Sotomayor, A.,; Stuchlik, Z., Isotropization and change of complexity by gravitational decoupling. *Eur. Phys. J. C* **2019**, *79*, 826.

[32] Tolman, R. C. Static Solutions of Einstein's Field Equations for Spheres of Fluid. *Phys. Rev.* **1939**, *55*, 364–373.